Paper

New building blocks for crystal engineering. Syntheses and crystal structures of oxime-substituted pyridines

Christer B. Aakeröy, Alicia M. Beatty and Destin S. Leinen

Department of Chemistry, Kansas State University, Manhattan, KS, 66506, USA. E-mail: aakeroy@ksu.edu

Received 26th July 2000, Accepted 5th September 2000
Published on the Web 18th September 2000

The syntheses and crystal structures of a family of oxime-substituted pyridine ligands [py-C(R)NOH, where R = H, Me, Ph, or NH_2] are presented. The compounds are all prepared in good yields by allowing a suitably substituted pyridine to react with hydroxylamine. Their solid-state structures show that the dominating hydrogen bond, a head-to-tail O–H···N interaction between the oxime O–H moiety and the pyridine nitrogen atom, is present in each of the seven reported cases. This intermolecular interaction generates infinite chains that are crosslinked into 2D or 3D assemblies by weaker C–H···N or C–H···O hydrogen bonds.

Introduction

The ability to predict and control the assembly of molecules and complex ions into extended ordered networks is an important goal in crystal engineering. Even though there are many inherent difficulties with using comparatively weak forces as primary synthetic tools, considerable progress has been made during the last decade.[1] In this context, the selectivity and directionality of the hydrogen bond have been instrumental in the preparation of distinctive structural aggregates,[2] and the use of hydrogen bonding as a steering force has emerged as the most important strategy in crystal engineering.[3] Despite recent advances, detailed control over the supramolecular assembly of molecules remains an elusive goal, and much more work is required to increase the choice of reliable building blocks of extended architectures held together by non-covalent forces.[4]

The oxime functionality is well known in organic synthesis,[5] analytical chemistry,[6] and coordination chemistry,[7–10] yet it has remained relatively unexplored as an intermolecular connector in crystal engineering.[11] However, recent work has shown how oxime pyridine derivatives can be utilized in the assembly of a variety of coordination complexes into extended networks.[12,13] By itself, the oxime moiety can, in the absence of other hydrogen bond donors/acceptors, generate several low-dimensional networks through hydrogen bonds. Adjacent moieties can form a head-to-head $R_2^2(6)$ motif (resulting in discrete dimers), or a catemeric motif that can lead to either discrete multi-molecular rings or infinite chains, Scheme 1.

From a crystal engineering perspective, the oxime moiety could be particularly appealing since it is electronically and sterically 'tunable'; *R* and *R*′ can be modified to include a wide range of electron donors/acceptors or 'inert' spacers, and these functional groups are accessible through well-known synthetic methods.[14]

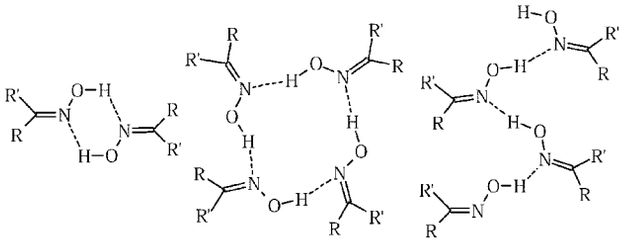

Scheme 1 Possible hydrogen bond motifs with oxime functionalities.

If the oxime functionality is attached to a moiety that can act as coordinating site for a metal ion, then a potential 'bridge' between coordination complexes and supramolecular assembly has been constructed, Scheme 2.

Previous data demonstrate that the oxime functionality does enable the assembly of silver(I) ions *via* the dimeric head-to-head interaction to infinite silver(I) chains that are further propagated into 2D sheets *via* C–H···O hydrogen bonds, Fig. 1.

The counter-ions are positioned between the cationic layers, and participate in weaker hydrogen bonds to the layer above and below. Structures of this type demonstrate that supramolecular synthesis using the oxime functionality can provide predictable structural arrangements where coordination complexes are directed into ordered networks by relatively weak forces working in concert. As part of this process, it is necessary to (i) synthesize and characterize a range of new ligands and (ii) to determine their solid-state behavior and hydrogen bond patterns in the absence of metal-ions. In this paper we present the syntheses of five oxime-substituted pyridine ligands, and the crystal structures of seven such compounds.

Experimental

Syn-2-aldoximepyridine, **1**, and 3-aldoximepyridine, **2**, and all starting materials were purchased from Aldrich and used as received without further purification. Melting points were determined using a Fisher-Johns Mel-Temp melting point apparatus and are uncorrected. ^{1}H NMR spectra were recorded on a Varian 400 MHz spectrometer. ^{13}C NMR spectra were recorded on a Varian 200 MHz spectrometer.

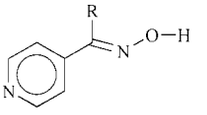

Scheme 2 Generic oxime-substituted pyridine ligand for crystal engineering of coordination complexes.

DOI: 10.1039/b006043g

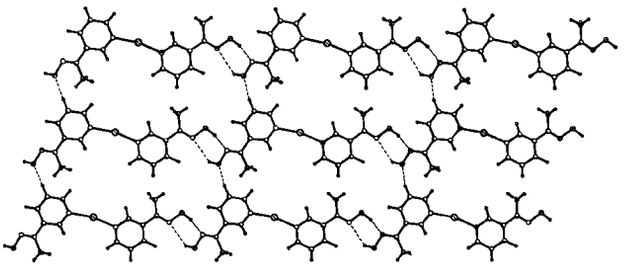

Fig. 1 Infinite cationic sheet in di(3-acetyloximepyridine)silver(I) hexafluorophosphate.

Crystallization of syn-2-aldoxime, 1, and 3-aldoximepyridine, 2

Slow evaporation of saturated solutions of **1** in 95% ethanol and **2** in absolute ethanol produced colorless rods and colorless needles, respectively, suitable for X-ray diffraction.

Synthesis of 3-acetyloximepyridine, 3

3-Acetylpyridine (4.00 g, 3.30 mmol) was dissolved in ethanol (30 ml) with stirring. $NH_2OH{\cdot}HCl$ (3.44 g, 4.95 mmol) in 30 ml distilled water and Na_2CO_3 (2.62 g, 24.8 mmol) in 50 ml distilled water were added to the ethanolic 3-acetylpyridine solution. The mixture was heated under reflux for 48 h. The resulting solution was concentrated under reduced pressure, producing a white precipitate. The vessel was cooled in an ice bath, and a white solid was collected *via* vacuum filtration. The precipitate was washed with small portions of cold water, and dried with an aspirator. Yield: 3.42 g (76%). Mp 118–120 °C. ^{1}H NMR: δ_H (400 MHz; DMSO-d_6) 2.15(3H, s), 7.37–7.40(1H, dd), 7.97–7.99(1H, d), 8.52–8.53(1H, d), 8.81(1H, s) and 11.45(1H, s). ^{13}C NMR: δ_C (200 MHz; DMSO-d_6) 11.4, 123.4, 132.4, 132.8, 146.5, 149.3 and 151.0. Colorless, irregular prisms suitable for X-ray diffraction were grown from a saturated solution of **3** in methylene chloride.

Synthesis of 4-acetyloximepyridine, 4

4-Acetylpyridine (4.00 g, 3.30 mmol) was dissolved in ethanol (30 ml) with stirring. $NH_2OH{\cdot}HCl$ (3.44 g, 4.95 mmol) in 30 ml distilled water and Na_2CO_3 (2.62 g, 24.8 mmol) in 50 ml distilled water were added to the ethanolic 4-acetylpyridine solution. The mixture was heated under reflux for 48 h. The resulting solution was concentrated under reduced pressure, producing a white precipitate. The vessel was cooled in an ice bath, and a white solid was collected *via* vacuum filtration. The precipitate was washed with small portions of cold water, and dried with an aspirator. Yield: 3.92 g (87%). Mp 157–158 °C. ^{1}H NMR: δ_H (400 MHz; DMSO-d_6) 2.13(3H, s), 7.57–7.58(2H, d), 8.54–8.56(2H, d) and 11.68(1H, s). ^{13}C NMR: δ_C (200 MHz; DMSO-d_6) 11.0, 119.8, 143.8, 149.7 and 151.4. Colorless, irregular prisms suitable for X-ray diffraction were grown from a saturated solution of **4** in methylene chloride.

Synthesis of 4-amidoximepyridine, 5

4-Cyanopyridine (2.00 g, 19.2 mmol) was dissolved in ethanol (20 ml) with stirring. $NH_2OH{\cdot}HCl$ (1.34 g, 19.2 mmol) in 10 ml distilled water and Na_2CO_3 (1.02 g, 9.61 mmol) in 25 ml distilled water were added to the ethanolic 4-cyanopyridine solution. The mixture was stirred overnight. The resulting brown solution was concentrated under reduced pressure, producing an off-white precipitate. The vessel was cooled in an ice bath, and an off-white precipitate was collected *via* vacuum filtration. The solid was washed with small portions of cold water, dried with an aspirator, and recrystallized from ethanol to yield off-white crystals. Yield: 1.41 g (54%). Mp 201–205 °C. ^{1}H NMR: δ_H (400 MHz; DMSO-d_6) 5.98(2H, s), 7.61–7.62(2H, d), 8.54–8.55(2H, d) and 10.04(1H, s). ^{13}C NMR: δ_C (200 MHz; DMSO-d_6) 119.5, 140.4, 148.7 and 149.5. Colorless prisms suitable for X-ray diffraction were grown from a saturated solution of **5** in absolute ethanol.

Synthesis of 4-benzoyloximepyridine, 6

4-Benzoylpyridine (4.00 g, 2.18 mmol) was dissolved in ethanol (40 ml) with stirring. $NH_2OH{\cdot}HCl$ (2.28 g, 3.27 mmol) in 20 ml distilled water and Na_2CO_3 (1.74 g, 16.4 mmol) in 45 ml distilled water were added to the ethanolic 4-benzoylpyridine solution. The mixture was stirred for 6 days to produce a white precipitate. The vessel was cooled in an ice bath, and a white solid collected *via* vacuum filtration. The precipitate was washed with small portions of cold water, and dried with an aspirator. Yield: 2.10 g (49%). Mp 184–188 °C. ^{1}H NMR: δ_H (400 MHz; DMSO-d_6) 7.29–7.31(2H, d), 7.38(5H, s), 8.68–8.69(2H, d) and 11.67(1H, s). ^{13}C NMR: δ_C (200 MHz; DMSO-d_6) 123.5, 126.6, 128.5, 129.2, 135.1, 141.2, 149.6 and 153.1. Colorless, rectangular prisms suitable for X-ray diffraction were grown from a saturated solution of **6** in methanol.

Synthesis of 3-benzoyloximepyridine, 7

3-Benzoylpyridine (2.00 g, 1.09 mmol) was dissolved in ethanol (25 ml) with stirring. $NH_2OH{\cdot}HCl$ (1.14 g, 1.64 mmol) in 20 ml distilled water and Na_2CO_3 (0.87 g, 8.19 mmol) in 40 ml distilled water were added to the ethanolic 3-benzoylpyridine solution. The mixture was heated under reflux for 48 h. Upon cooling to room temperature, a white precipitate appeared. The solution was concentrated under reduced pressure, then cooled in an ice bath. A white precipitate was collected *via* vacuum filtration, washed with small portions of cold water, and dried with an aspirator. Recrystallization from ethanol gave white crystals. Yield: 1.76 g (81%). Mp 154–157 °C. ^{1}H NMR: δ_H (400 MHz; DMSO-d_6) 7.37(5H, s), 7.46–7.50(1H, m), 7.69–7.72(1H, d), 8.47(1H, s), 8.58–8.60(1H, d) and 11.59(1H, s). ^{13}C NMR: δ_C (200 MHz; DMSO-d_6) single isomer: 123.4, 126.8, 128.4, 129.1, 129.2, 135.9, 136.6, 149.1, 149.2, and 152.6; mixture of isomers: 123.4, 126.8, 128.3, 128.5, 128.7, 128.8, 129.1, 129.2, 129.7, 132.4, 132.5, 134.3, 135.9, 136.6, 147.6, 149.1, 149.3, 149.5, 152.7, and 153.0. Colorless prisms suitable for X-ray diffraction were grown from a saturated solution of **7** in acetone.

X-ray crystallography

Crystal data for **1**–**7** were collected using a Siemens P4 four-circle diffractometer with graphite monochromated Mo-Kα ($\lambda = 0.71073$ Å) radiation at 173 K. Cell parameters were obtained from 35 accurately centered reflections in the 2θ range 10–28°. Data were collected using a θ–2θ scanning technique, and Lorentz and polarization corrections were applied. The structures were solved by direct methods, with non-hydrogen atoms found by successive full matrix least squares refinement on F^2 and refined with anisotropic thermal parameters. Hydrogen atom positions were located from difference Fourier maps, and a riding model with fixed thermal parameters [$u_{ij} = U_{ij}$(eq) for the atom to which they are bonded] was used for subsequent refinements. The weighting function applied was $w^{-1} = [\sigma^2(F_o^2) + (g_1P)^2 + (g_2P)]$ where $P = [F_o^2 + 2F_c^2]/3$. The SHELXTL PC and SHELXL-93 packages were used for data reduction and structure solution and refinement.[15] Tables 1–3 provide crystallographic details for **1**–**7**, and the molecular geometries and numbering schemes are shown in Fig. 2.

Results

There are two unique molecules in the asymmetric unit of **1**. The molecules, related by a 2_1 screw axis, form infinite 1D chains held together by hydrogen bonds. The predominant

Table 1 Crystal data and refinement for **1**–**3** [a]

Crystal data	**1**	**2**	**3**
Empirical formula	$C_6H_6N_2O$	$C_6H_6N_2O$	$C_7H_8N_2O$
M	122.13	122.13	136.15
Crystal size/mm^3	$0.62 \times 0.36 \times 0.24$	$0.24 \times 0.22 \times 0.22$	$0.46 \times 0.40 \times 0.28$
Crystal system	Monoclinic	Orthorhombic	Monoclinic
Space group	*P*2(1)/*c*	*Pna*2(1)	*C*2/*c*
a/Å	16.407(2)	19.014(2)	12.8175(9)
b/Å	8.4341(7)	3.8296(4)	9.627(2)
c/Å	9.0196(8)	8.1179(8)	11.420(1)
α/°	90	90	90
β/°	105.758(7)	90	91.918(6)
χ/°	90	90	90
V/Å^3	1201.2(2)	591.1(1)	1408.4(3)
Z	8	4	8
μ(Mo-Kα)/mm^{-1}	0.096	0.098	0.089
T/K	173(2)	173(2)	173(2)
Reflections collected	2253	1103	1090
Unique reflections	2102	815	1039
Observed reflections ($I > 2\sigma I$)	1399	639	893
R/R_w^2 (obs. data)	0.0481/0.1091	0.0446/0.0900	0.0418/0.1085
R/R_w^2 (all data)	0.0825/0.1248	0.0646/0.0982	0.0487/0.1135

[a]Click here for full crystallographic data (CCDC no. 1350/33).

Table 2 Crystal data and refinement for **4**–**6**[a]

Crystal data	**4**	**5**	**6**
Empirical formula	$C_7H_8N_2O$	$C_6H_7N_3O$	$C_{12}H_{10}N_2O$
M	136.15	137.15	198.22
Crystal size/mm^3	$0.42 \times 0.38 \times 0.34$	$0.65 \times 0.54 \times 0.36$	$0.40 \times 0.20 \times 0.20$
Crystal system	Monoclinic	Orthorhombic	Monoclinic
Space group	*P*2(1)/*c*	*Pna*2(1)	*P*2(1)/*c*
a/Å	6.3502(7)	12.5433(6)	5.7943(6)
b/Å	14.296(1)	8.7821(9)	17.615(2)
c/Å	7.6172(7)	5.7857(4)	10.271(1)
α/°	90	90	90
β/°	91.622(5)	90	99.290(8)
χ/°	90	90	90
V/Å^3	691.2(1)	637.33(8)	1034.6(2)
Z	4	4	4
μ(Mo-Kα)/mm^{-1}	0.091	0.103	0.083
T/K	173(2)	173(2)	173(2)
Reflections collected	1717	803	2004
Unique reflections	1584	803	1817
Observed reflections ($I > 2\sigma I$)	1159	775	1251
R/R_w^2 (obs. data)	0.0521/0.1312	0.0286/0.0779	0.0507/0.1027
R/R_w^2 (all data)	0.0756/0.1454	0.0300/0.0786	0.0860/0.1169

[a]Click here for full crystallographic data (CCDC no. 1350/33).

hydrogen bond interaction assembling the chains is a head-to-tail O–H···N hydrogen bond involving the oxime O–H and the pyridine nitrogen atom [O7–N1 = 2.787(3) Å; O27–N21 = 2.785(3) Å], Fig. 3. There is also a C–H···N hydrogen bond involving the oxime C–H and the oxime nitrogen atom [C7–N7 = 3.274(3)Å; C(27)–N(27) = 3.283(3) Å]. The chains are arranged in an *anti*-parallel fashion and pack in a typical herringbone motif.

In the crystal structure of **2**, infinite 1D chains are assembled through a head-to-tail O–H···N hydrogen bond involving the oxime O–H and the pyridine nitrogen atom [O7–N1 = 2.717(3) Å]. Adjacent chains are related by a glide plane, and the two chains are linked through a C–H···O [C2–O7 = 3.450(3) Å] hydrogen bond to form a 1D ribbon, Fig. 4. The ribbons are arranged in a herringbone motif and are hydrogen bonded to neighboring ribbons *via* C–H···N [C5–N7 = 3.659(4) Å] interactions to produce an overall 3D hydrogen bonded structure. All the oxime moieties within a ribbon point in the same direction, and all the ribbons, in turn, are aligned in a parallel fashion.

In the structure of **3**, the molecules form infinite 1D chains assembled through a head-to-tail O–H···N hydrogen bond

Table 3 Crystal data and refinement for **7**[a]

Crystal data	**7**
Empirical formula	$C_{12}H_{10}N_2O$
M	198.22
Crystal size/mm^3	$0.50 \times 0.25 \times 0.06$
Crystal system	Monoclinic
Space group	*P*2(1)/*n*
a/Å	5.649(1)
b/Å	12.737(2)
c/Å	14.507(2)
α/°	90
β/°	96.33(1)
χ/°	90
V/Å^3	1037.4(3)
Z	4
μ(Mo-Kα)/mm^{-1}	0.083
T/K	173(2)
Reflections collected	2614
Unique reflections	2382
Observed reflections ($I > 2\sigma I$)	1084
R/R_w^2 (obs. data)	0.0820/0.1795
R/R_w^2 (all data)	0.1842/0.2279

[a]Click here for full crystallographic data (CCDC no. 1350/33).

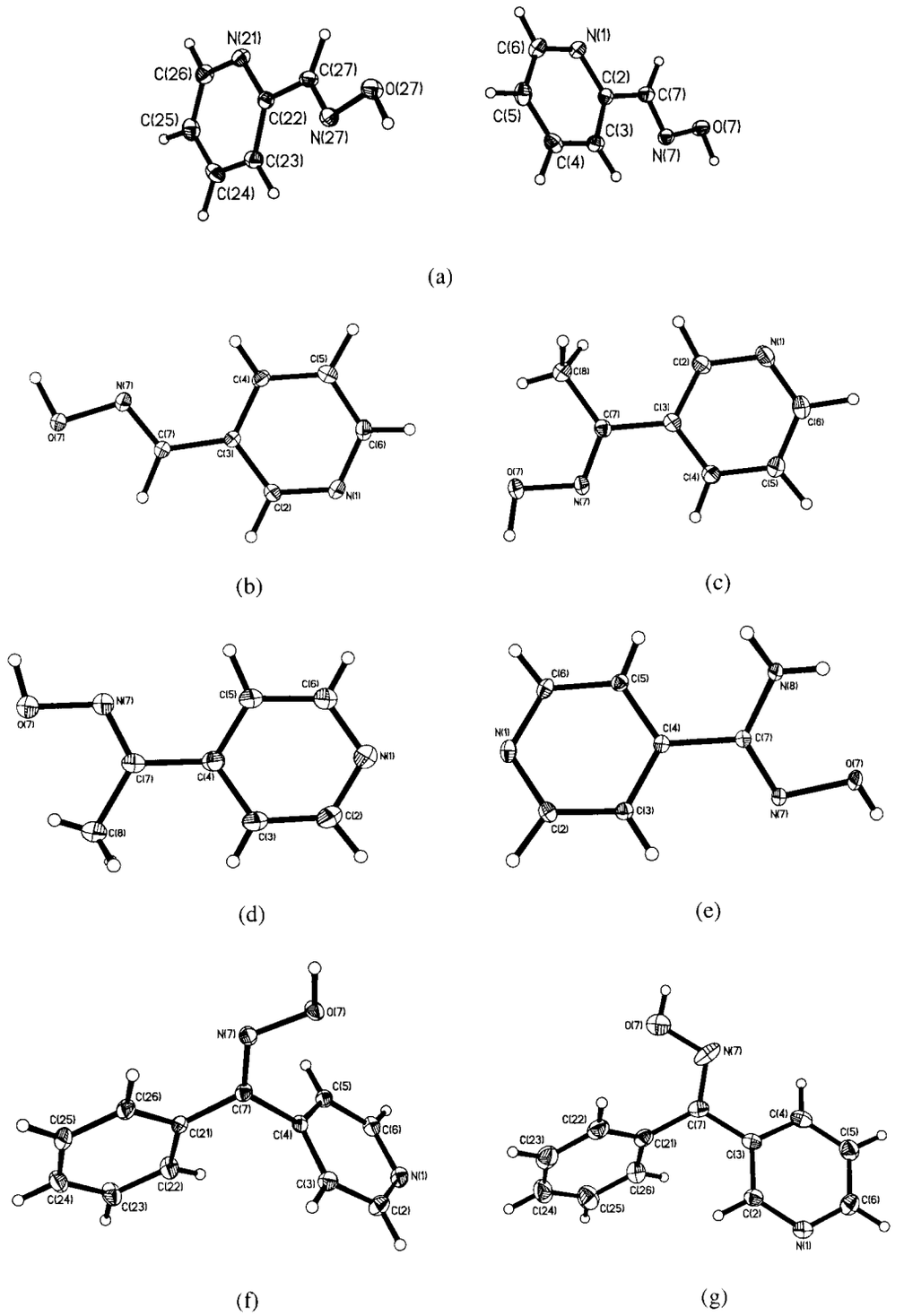

Fig. 2 Thermal ellipsoid plots of (a) 2-aldoximepyridine, **1**; (b) 3-aldoximepyridine, **2**; (c) 3-acetyloximepyridine, **3**; (d) 4-acetyloximepyridine, **4**; (e) 4-amidoximepyridine, **5**; (f) 4-benzoyloximepyridine, **6**; and (g) 3-benzoyloximepyridine, **7**. Click images or compound numbers to access 3D representations.

involving the oxime O–H and the pyridine nitrogen atom [O7–N1 = 2.720(2) Å], Fig. 5. Additional C–H···N [C4–N7 = 3.481(2) Å] and C–H···O [C5–O7 = 3.246(2) Å] hydrogen bonds cross-link the 1D chains to produce a 3D hydrogen bonded infinite architecture.

The crystal structure of **4** contains infinite 1D molecular chains assembled through a head-to-tail O–H···N hydrogen bond involving the oxime O–H and the pyridine nitrogen atom [O7–N1 = 2.711(2) Å]. The molecules comprising the chains are related by a 2_1 screw axis. Neighboring chains run *anti*-parallel to each other, Fig. 6. The chains are cross-linked *via* C–H···O hydrogen bonds [C6–O7 = 3.360(2) Å] resulting in 2D sheets. These sheets, which lie in the *ac* plane, stack to produce a lamellar structure. There are no hydrogen bond interactions between sheets.

The crystal structure of **5** also contains infinite 1D chains assembled through a head-to-tail O–H···N hydrogen bond involving the oxime O–H and the pyridine nitrogen atom [O7–N1 = 2.745(2) Å]. The chains are cross-linked *via* C–H···N hydrogen bonds [C2–N8 = 3.682(2) Å] involving a pyridine C–H and the nitrogen atom of the amino group attached to the oxime functionality. This interaction results in the formation of

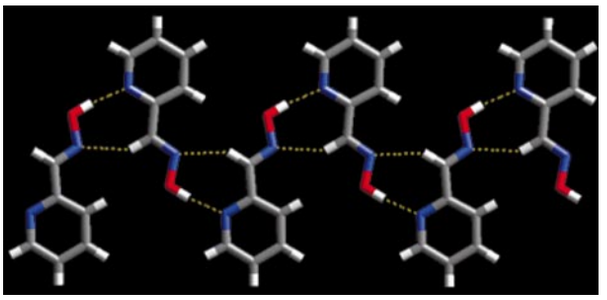

Fig. 3 Infinite chain of 2-aldoximepyridine, **1**. Click image or here to access 3D representation.

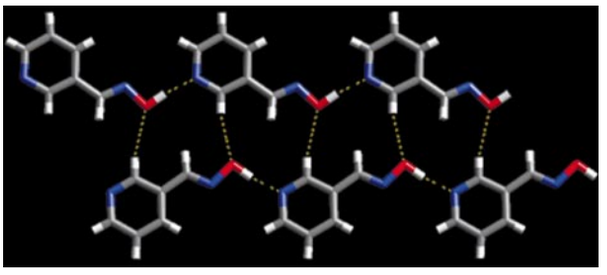

Fig. 4 Infinite ribbon of 3-aldoximepyridine, **2**. Click image or here to access 3D representation.

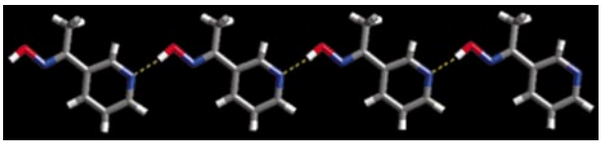

Fig. 5 Infinite 1D chain of 3-acetyloximepyridine, **3**. Click image or here to access 3D representation.

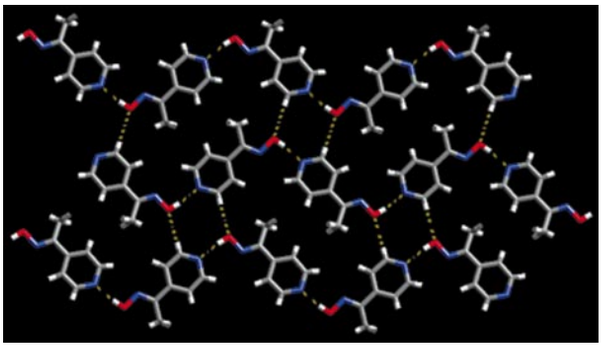

Fig. 6 Infinite sheets of 4-acetyloximepyridine, **4**. Click image or here to access 3D representation.

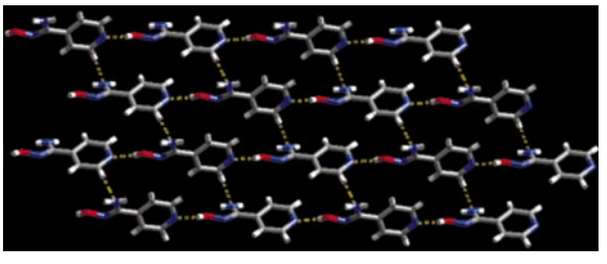

Fig. 7 Infinite 2D sheet in 4-amidoximepyridine, **5**. Click image or here to access 3D representation.

infinite 2D sheets, Fig. 7. The sheets have a corrugated appearance and stack together. The 2D sheets are propagated into a 3D structure by additional N–H···N hydrogen bonds between the amino N–H and the oxime nitrogen atom [N8–N7 = 3.090(2) Å]. The overall structure is a 3D hydrogen bonded architecture.

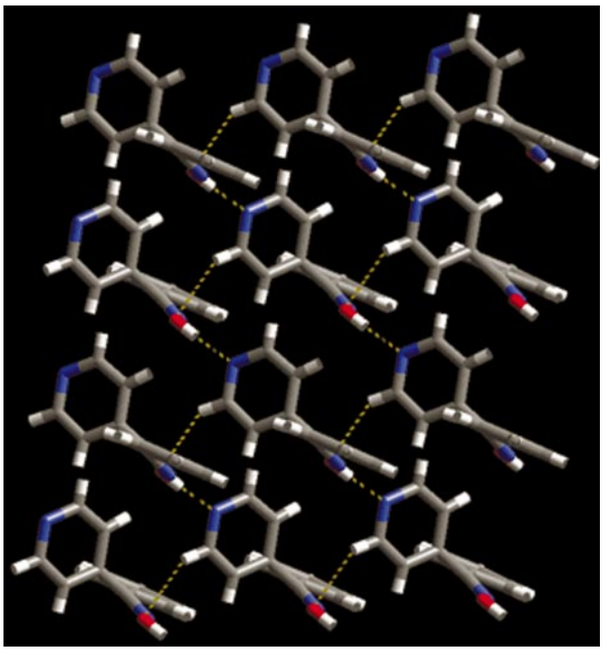

Fig. 8 Infinite 2D sheet in 4-benzoyloximepyridine, **6**. Click image or here to access 3D representation.

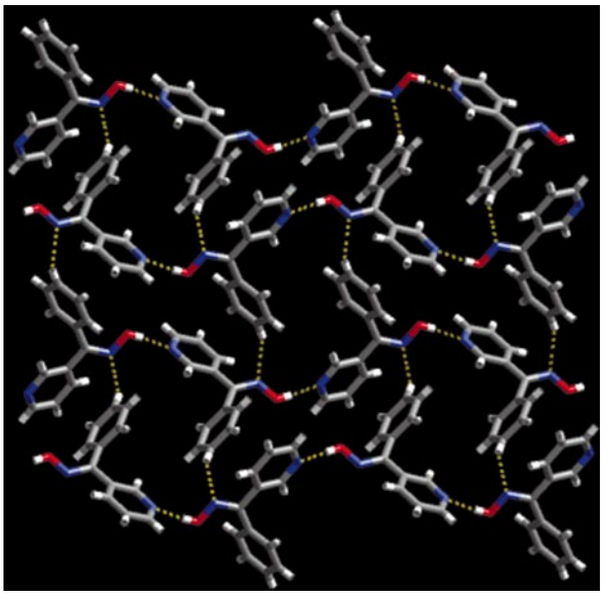

Fig. 9 Infinite 2D sheet in 3-benzoyloximepyridine, **7**. Click image or here to access 3D representation.

In **6**, the molecules form infinite 1D chains assembled through a head-to-tail O–H···N hydrogen bond involving the oxime O–H and the pyridine nitrogen atom [O7–N1 = 2.749(2) Å]. Molecules within each chain are related by a 2_1 screw axis. Neighboring chains run parallelly, and are cross-linked by C–H···O hydrogen bonds [C6–O7 = 3.278(3) Å] to generate infinite 2D sheets, Fig. 8. The phenyl rings protrude above and below the corrugated 2D sheets and interdigitate as a result of close-packing; however, there are no short aryl–aryl contacts or hydrogen bonding interactions between sheets.

Finally, in **7**, the molecules form infinite 1D chains assembled through a head-to-tail O–H···N hydrogen bond involving the oxime O–H and the pyridine nitrogen atom

[O(7)–N(1) = 2.737(4) Å]. The molecules within each chain are related by a 2_1 screw axis. The chains are cross-linked by C–H···N hydrogen bonds involving a phenyl C–H and the oxime nitrogen atom [C(24)–N(7) = 3.509(6) Å] to form infinite corrugated sheets, Fig. 9. The chains comprising each sheet run in an *anti*-parallel fashion. The corrugated sheets stack in a tongue-and-groove manner as a result of close packing; however, there are no hydrogen bonds between sheets.

Discussion

Compounds **3**–**7** were synthesized in moderate to good yields by allowing the appropriate substituted pyridine to react with hydroxylamine. The chemical shifts, splitting patterns, and integration in the ^{1}H-NMR spectra of **3**–**7** supported the identities of the desired compounds and no trace of starting material was observed in the spectra. The ^{1}H-NMR and ^{13}C-NMR spectra of the crude compounds revealed that **3**–**6** were isolated as single isomers, whereas **7** was isolated as a mixture of geometrical isomers. A single isomer of **7** was obtained by recrystallization from ethanol.

The crystal structures for **1**–**7** show that all the molecules have the *antiperiplanar* conformation, with C=N–O–H torsion angles in the range of 166–180°. This conformation is more stable than the *synplanar* conformation and is also required for hydrogen bond formation. In addition, all molecules, except **6**, display a configuration where the oxime O–H is *trans* to the pyridyl ring.

The dominating intermolecular interaction in all structures is a head-to-tail hydrogen bond from the oxime moiety to the pyridine nitrogen atom. Regardless of the R substituent of the oxime functionality (–H, –CH_3, –NH_2, or Ph), this interaction prevails and generates infinite 1D molecular chains in **1**–**7**. A search of the CSD[16] found other pyridineoxime derivatives[17] where the same head-to-tail hydrogen bond is present in each case. More recently, two other oxime-substituted pyridines were also reported to display the very same interaction.[18] This supports the conclusion that the pyridine nitrogen atom is a better hydrogen bond acceptor than the oxime nitrogen atom in these molecules.

While changing the nature of the *R* substituent does not affect the principle structural motif (*i.e.* chain formation) in **1**–**7**, it does play a role in determining the structural outcome. This secondary influence may be attributed more to steric, rather than electronic, factors. For example, 3-aldoximepyridine crystallizes in the orthorhombic space group $Pna2_1$, while 3-acetyloximepyridine crystallizes in the monoclinic space group $C2/c$.

We have shown that pyridineoximes form infinite 1D chains in the solid-state assembled *via* a head-to-tail O–H···N hydrogen bond between the oxime O–H and the pyridine nitrogen atom. Although many options for assembly are possible (Scheme 1), the primary motif (*i.e.* chain formation) remains intact and dominates the crystal structures of **1**–**7**. The O–H···N interaction not only reaffirms the notion of the best hydrogen bond donor pairing with the best acceptor,[19] but also demonstrates the ability of a stronger hydrogen bond to dictate the structural outcome over weaker C–H···A interactions.

We have previously demonstrated the utility of the pyridineoximes as 'building blocks' ideally suited for the supramolecular synthesis of inorganic–organic hybrid materials due to the consistency in their primary hydrogen bond interactions (*i.e.* dimer formation). This work opens avenues into the organic solid-state, as the persistence of the O–H···N hydrogen bond provides for the controlled and predictable assembly of compounds displaying both oxime and pyridyl moieties.

Acknowledgements

We are grateful for financial support from NSF (CHE-0078996) and Kansas State University.

References

1 (*a*) G. R. Desiraju, *Crystal Engineering: The Design of Organic Solids*, Elsevier, Amsterdam, 1989.; (*b*) J.-M. Lehn, *Supramolecular Chemistry*, VCH, Weinheim, 1995.; (*c*) C. B. Aakeröy, *Acta Crystallogr., Sect. B*, 1997, **B53**, 569; (*d*) *Perspectives in Supramolecular Chemistry, Vol. 2, The Crystal as a Supramolecular Entity*, ed. G. R. Desiraju, Wiley, Chichester, 1995.

2 (*a*) R. Thaimattam, D. S. Reddy, F. Xue, T. C. W. Mak, A. Nangia and G. R. Desiraju, *J. Chem. Soc., Perkin Trans.*, 1998, 1783; (*b*) P. R. Ashton, M. C. T. Fyfe, S. K. Hickingbottom, S. Menzer, J. F. Stoddart, A. J. P. White and D. J. Williams, *Chem. Eur. J.*, 1998, **4**, 577; (*c*) S. V. Kolotuchin and S. C. Zimmerman, *J. Am. Chem. Soc.*, 1998, **120**, 9092; (*d*) K. Kobayashi, T. Shirasaka, K. Yamaguchi, S. Sakamoto, E. Horn and N. Furukawa, *Chem. Commun.*, 2000, 41; (*e*) D. E. Lynch, S. Chatwin and S. Parsons, *Cryst. Eng.*, 1999, **2**, 137; (*f*) C. B. Aakeröy and M. Nieuwenhuyzen, *J. Am. Chem. Soc.*, 1994, **116**, 10983; (*g*) C. B. Aakeröy, D. P. Hughes and M. Nieuwenhuyzen, *J. Am. Chem. Soc.*, 1996, **118**, 10134; (*h*) J. A. Swift, A. M. Pivovar, A. M. Reynolds and M. D. Ward, *J. Am. Chem. Soc.*, 1998, **120**, 5887.

3 (*a*) V. A. Russell and M. D. Ward, *Chem. Mater.*, 1996, **8**, 1654; (*b*) C. B. Aakeröy and K. R. Seddon, *Chem. Soc. Rev.*, 1993, **22**, 397; (*c*) S. Subramanian and M. Zaworotko, *Coord. Chem. Rev.*, 1994, **137**, 357.

4 G. R. Desiraju, *Angew. Chem., Int. Ed. Engl.*, 1995, **34**, 2311.

5 J. P. Freeman, *Chem. Rev.*, 1973, **73**, 283.

6 N. M. Samus and A. V. Ablov, *Coord. Chem. Rev.*, 1979, **28**, 177.

7 V. Y. Kukushkin, D. Tudela and A. J. L. Pombeiro, *Coord. Chem. Rev.*, 1996, **156**, 333.

8 S. Kawata, S. Kitagawa, H. Machida, T. Nakamoto, M. Kondo, K. Katada, K. Kikuchi and I. Ikemoto, *Inorg. Chim. Acta*, 1995, **229**, 211.

9 V. Yu, T. Nishioka, D. Tudela, K. Isobe and A. J. L. Pombeiro, *Coord. Chem. Rev.*, 1996, **156**, 333.

10 K. Isobe and I. Kinoshita, *Inorg. Chem.*, 1997, **36**, 6157.

11 (*a*) F. J. Hoogesteger, L. W. Jenneskens, H. Kooijman, N. Veldman and A. J. Spek, *Tetrahedron*, 1996, **52**, 1773; (*b*) K. Y. Lau, A. Mayr and K.-K. Cheung, *Inorg. Chim. Acta*, 1999, **285**, 223; (*c*) A. W. Marsman, PhD Thesis, Utrecht University, 1999.; (*d*) L. Chertanova, C. Pascard and A. Sheremetev, *Acta Crystallogr., Sect. B*, 1994, **B50**, 708.

12 C. B. Aakeröy, A. M. Beatty and D. S. Leinen, *Angew. Chem., Int. Ed.*, 1999, **38**, 1815.

13 C. B. Aakeröy, A. M. Beatty and D. S. Leinen, *J. Am. Chem. Soc.*, 1998, **120**, 7383.

14 (*a*) T. Katagi, H. Kataoka, K. Takahashi, T. Fujioka, M. Kunitomo, Y. Yamaguchi, M. Fujiwara and T. Inoi, *Chem. Pharm. Bull.*, 1992, **40**, 2419; (*b*) T. Kato, Y. Goto and T. Chiba, *Yakugaku Zasshi*, 1967, **87**, 689; (*c*) H. Adkins, I. A. Wolff, A. Pavlic and E. Hutchinson, *J. Am. Chem. Soc.*, 1944, **66**, 1293; (*d*) E. Bernasek, *J. Org. Chem.*, 1957, **22**, 1263; (*e*) G. Massolini, M. Kitsos, C. Gandini and G. Caccialanza, *Pestic. Sci.*, 1989, **26**, 209; (*f*) G. Massolini, M. L. Carmellino and A. Baruffini, *Farmaco Ed. Sci.*, 1987, **42**, 117.

15 SHELXTL PC and SHELXL-93, G. M. Sheldrick, University of Göttingen, 1993.

16 Cambridge Structural Database, ver. 5.18; Cambridge Crystallographic Data Centre, 12 Union Road, Cambridge, England.

17 (*a*) M. Martínez-Ripoll and H. P. Lorentz, *Acta Crystallogr., Sect. B*, 1976, **B32**, 2322; (*b*) M. Martínez-Ripoll and H. P. Lorentz, *Acta Crystallogr., Sect. B*, 1976, **B32**, 2325; (*c*) J. M. Sorof, H. L. Carrell, J. P. Glusker, J. McLick and E. Kun, *Acta Crystallogr., Sect. C*, 1985, **C41**, 785; (*d*) Z. G. Aliev, V. G. Kartsev and L. O. Atovmyan, *Zh. Strukt. Khim.*, 1991, **32**, 113–3; (*e*) N. Okabe and M. Akita, *Acta Crystallogr., Sect. C*, 1997, **C53**, 1324; (*f*) T. Taga, A. Uchiyama, K. Machida and T. Miyasaka, *Acta Crystallogr., Sect. C*, 1990, **C46**, 2241.

18 (*a*) M. Mazik, D. Bläser and R. Boese, *Tetrahedron Lett.*, 1999, **40**, 4783; (*b*) M. Mazik, D. Bläser and R. Boese, *Tetrahedron*, 1999, **55**, 7835.

19 M. C. Etter, *J. Phys. Chem.*, 1991, **95**, 4601.